# Fig. S1

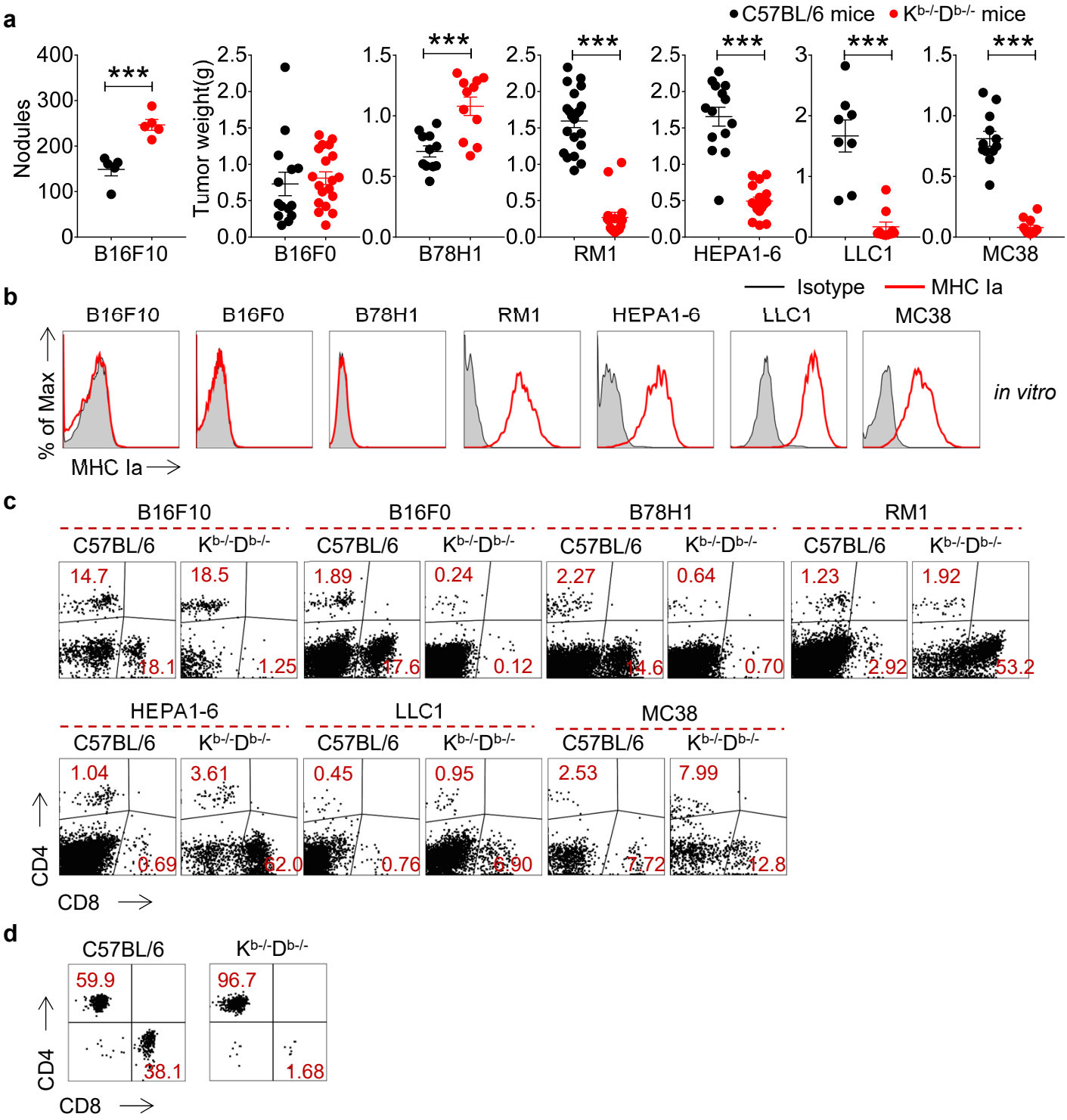


**Fig. S1. The presence of MHC Ia inhibits tumor growth in $K^{b-/-}D^{b-/-}$ mice, related to Fig. 1.**

(a) C57BL/6 and $K^{b-/-}D^{b-/-}$ mice were inoculated with B16F10 cells ($3\times10^5$, i.v.) and other tumor cells ($2\times10^5$, i.m.) to evaluate tumor burden.

(b) Analysis of MHC Ia expression levels on B16F10, B16F0, B78H1, RM1, HEPA1-6, LLC1, and MC38 by flow cytometry. Tumor cells were harvested from cell culture dishes.

(c) C57BL/6 and $K^{b-/-}D^{b-/-}$ mice were inoculated with B16F10 cells ($3\times10^5$, i.v.) and other tumor cells ($2\times10^5$, i.m.) and T cell infiltration were examined by flow cytometry.

(d) The percentage of $CD8^+$ T cells in splenic T cells of normal healthy C57BL/6 mice and $K^{b-/-}D^{b-/-}$ mice.

Data are presented as Mean±SEM. ***p<0.001.

# Fig. S2

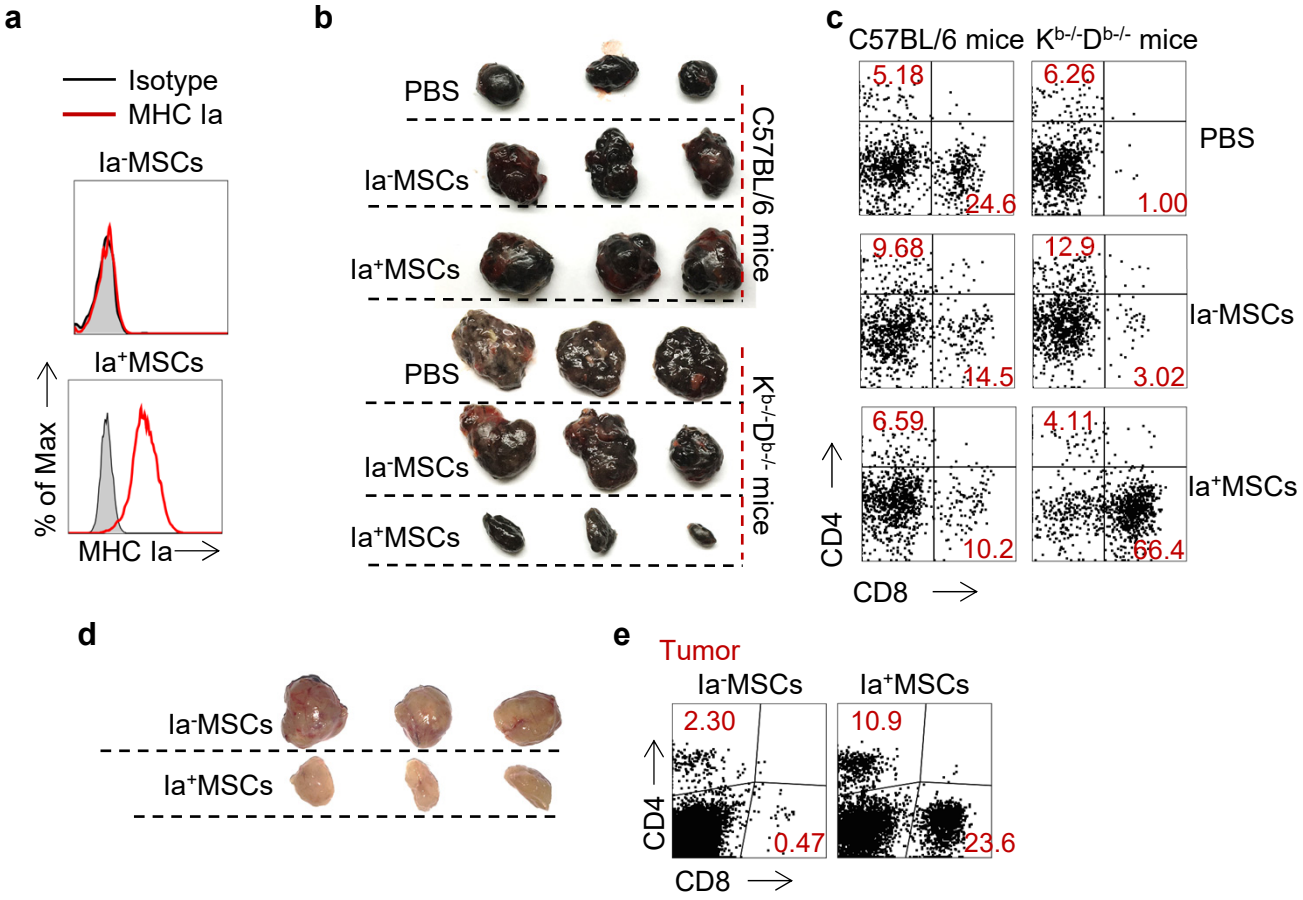


**Fig. S2. Co-injection of MHC Ia$^+$ cells inhibits tumor growth in K$^{b-/-}$D$^{b-/-}$ mice, related to Fig. 1.**

(a) The expression levels of MHC Ia on mesenchymal stromal cells isolated from K$^{b-/-}$D$^{b-/-}$ mice (Ia$^-$MSCs) or C57BL/6 mice (Ia$^+$MSCs) were determined by flow cytometry.

(b-c) B16F0 cells ($2\times10^5$) were i.m. administrated into C57BL/6 or K$^{b-/-}$D$^{b-/-}$ mice alone or with mesenchymal stromal cells ($2\times10^5$) derived from C57BL/6 mice (Ia$^+$MSCs) or K$^{b-/-}$D$^{b-/-}$ mice (Ia$^-$MSCs). The mice were euthanized on day 13 post tumor inoculation to evaluate tumor burden (b) and CD8$^+$ T cell infiltration at the tumor sites (c).

(d-e) B78H1 cells ($2\times10^5$) were co-administrated with Ia$^-$MSCs ($2\times10^5$) or Ia$^+$MSCs ($2\times10^5$) to K$^{b-/-}$D$^{b-/-}$ mice by i.m. injections. The mice were euthanized on day 13 post tumor inoculation to evaluate tumor burden (d) and CD8$^+$ T cell infiltration at the tumor sites (e).

# Fig. S3

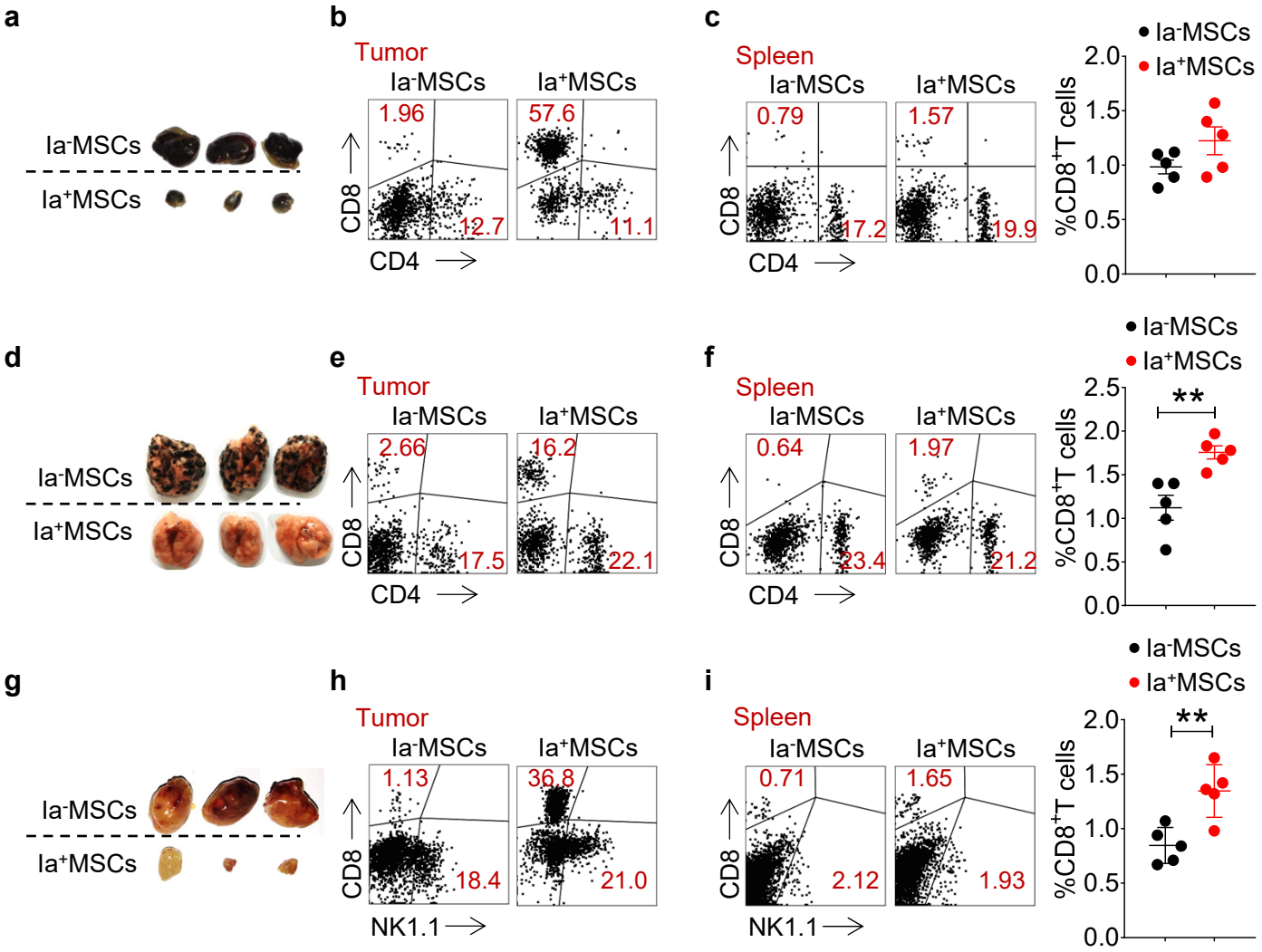


**Fig. S3. Administration of Ia$^+$MSCs intraperitoneally inhibits tumor growth in K$^{b-/-}$D$^{b-/-}$ mice, related to Fig. 1.**

(a-c) Ia$^+$MSCs or Ia$^-$MSCs were i.p administrated to K$^{b-/-}$D$^{b-/-}$ mice with i.m. inoculated B16F0. The size of tumor and the representative flow cytometry data of tumor infiltrated or splenic CD4$^+$ T cells and CD8$^+$ T cells were depicted.

(d-f) Ia$^+$MSCs or Ia$^-$MSCs were i.p administrated to K$^{b-/-}$D$^{b-/-}$ mice with i.v. inoculated B16F10. The lungs and the representative flow cytometry data of tumor infiltrated or splenic CD4$^+$ T cells and CD8$^+$ T cells were depicted.

(g-i) Ia$^+$MSCs or Ia$^-$MSCs were i.p administrated to K$^{b-/-}$D$^{b-/-}$ mice with i.m. inoculated B78H1. The size of tumor and the representative flow cytometry data of tumor infiltrated or splenic NK1.1$^+$ cells and CD8$^+$ T cells were depicted.

Data are presented as Mean±SEM. **p<0.01.

# Fig. S4

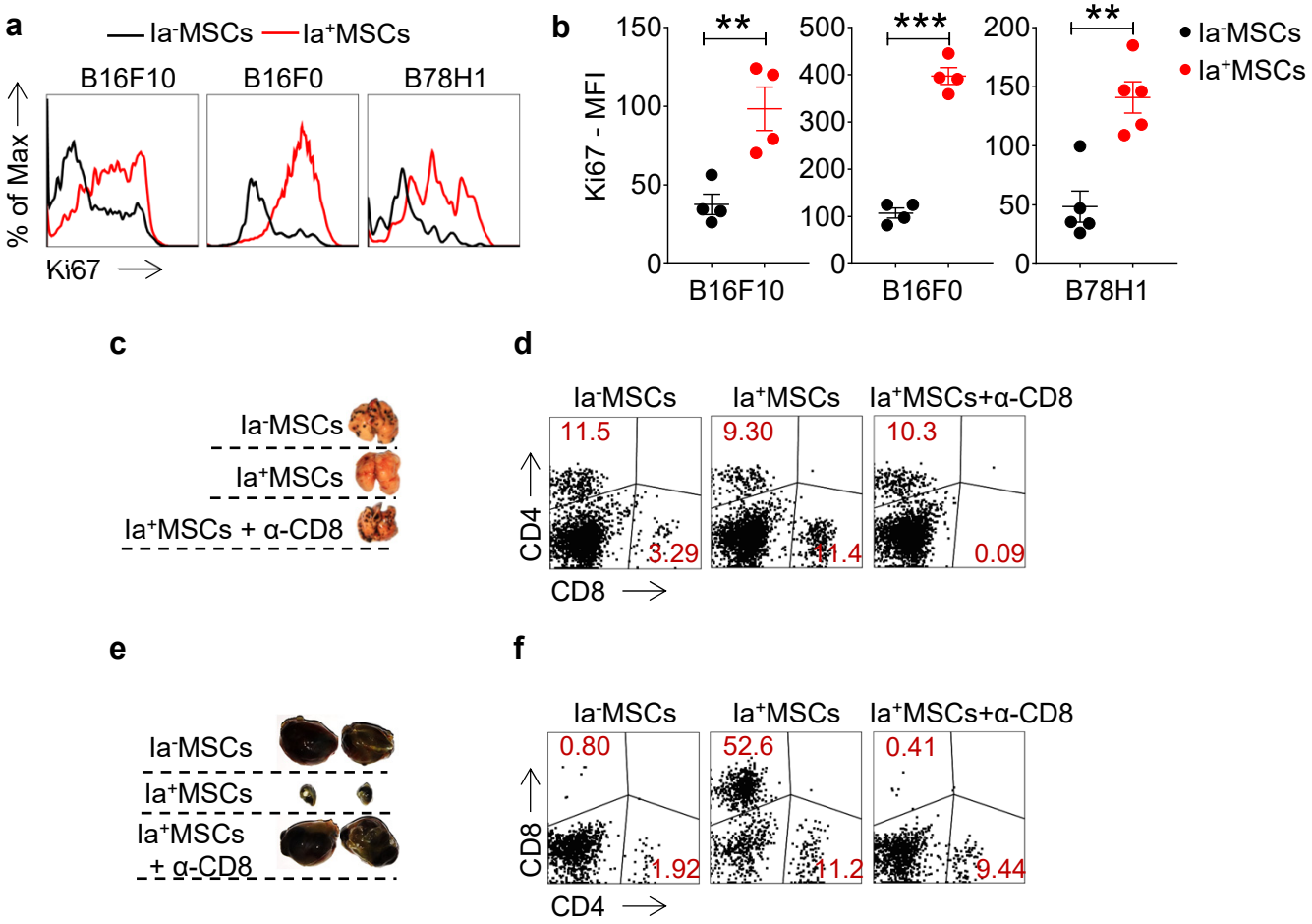


**Fig. S4. Ib-CD8$^+$ T cells mediate the tumor suppression effects of Ia$^+$MSCs, related to Fig. 1.**

(a-b) Ia$^+$MSCs or Ia$^-$MSCs were i.p administrated to K$^{b-/-}$D$^{b-/-}$ mice with B16F0 ($2\times10^5$, i.m.), B16F10 ($3\times10^5$, i.v.), or B78H1 ($2\times10^5$, i.m.) inoculations. The Ki67 expression on tumor infiltrated CD8$^+$ T cells was determined by flow cytometry.

(c-f) CD8 depletion antibodies (clone No: 2.43, 200 μg/mouse) were co-administrated together with Ia$^+$MSCs to B16F0 (c-d) or B16F10 (e-f) tumor bearing mice. Tumor burden and the representative flow cytometry data of tumor infiltrated CD4$^+$ T cells and CD8$^+$ T cells were shown.

Data are presented as Mean±SEM. **p<0.01, ***p<0.001.

# Fig. S5

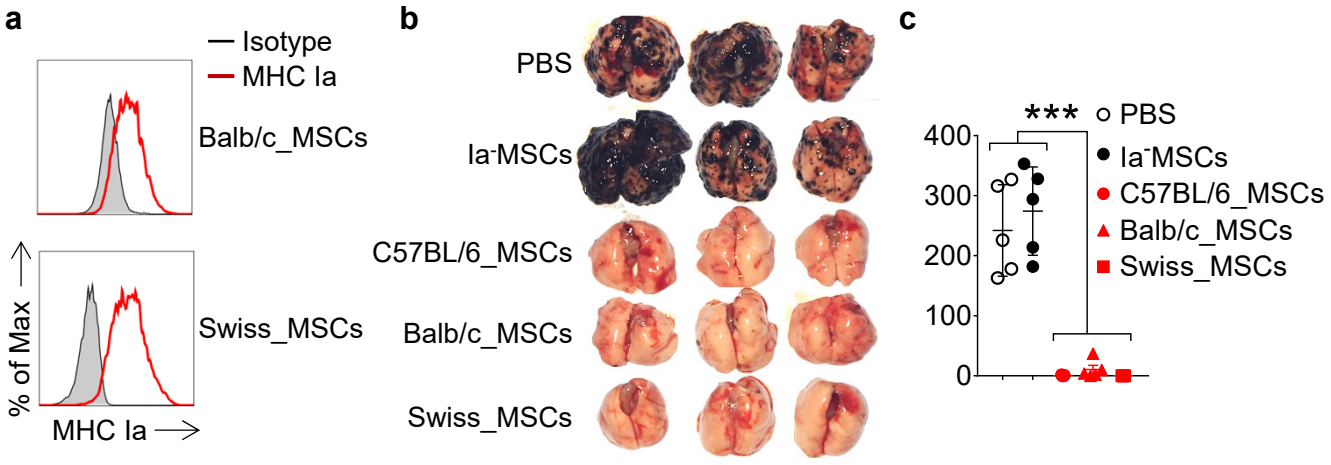


**Fig. S5. Tumor suppression effects of Ia$^{+}$MSCs in K$^{b-/-}$D$^{b-/-}$ mice are not dependent on MHC haplotypes, related to Fig. 1.**

(a-c) Mesenchymal stromal cells isolated from C57BL/6 (K$^{b}$D$^{b}$) (C57BL/6_MSCs), Balb/c (K$^{d}$D$^{d}$L$^{d}$) (Balb/c_MSCs), and Swiss (K$^{q}$D$^{q}$L$^{q}$) (Swiss_MSCs) mice were administrated to B16F10 tumor bearing K$^{b-/-}$D$^{b-/-}$ mice. The expression levels of MHC Ia on Balb/c_MSCs and Swiss_MSCs were analyzed (a). The tumor burdens in lungs were determined (b-c). Data are presented as Mean±SEM. ***p<0.001.

# Fig. S6

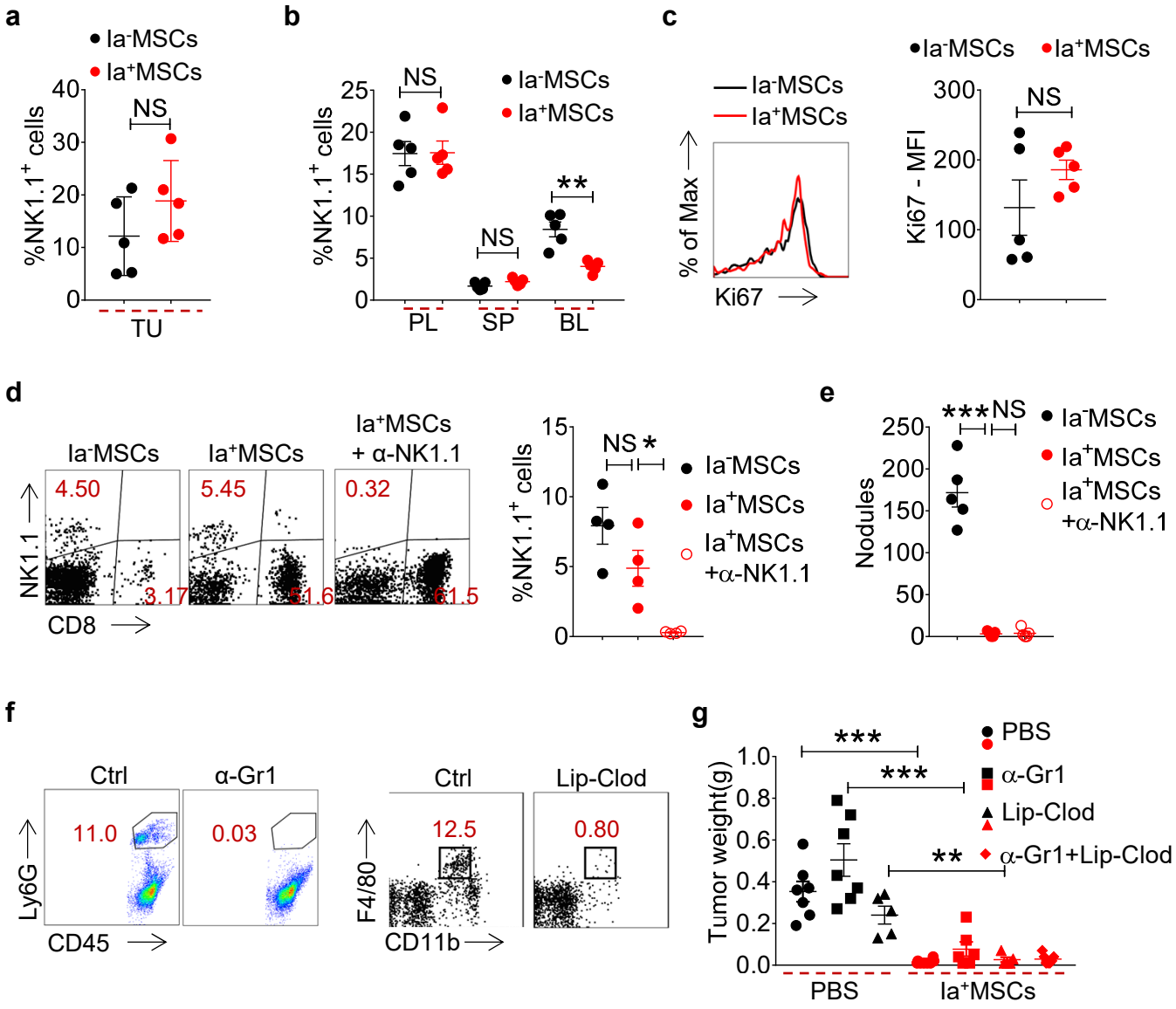


**Fig. S6. NK cells and myeloid cells are not involved in MHC Ia-mediated Ib-CD8$^+$ T cell expansion and tumoricidal effects, related to Fig. 1.**

(a-c) Ia$^+$MSCs or Ia$^-$MSCs were i.p. administrated to K$^{b-/-}$D$^{b-/-}$ mice with i.v. injected B16F10. The percentage of NK1.1$^+$ cells in tumor (TU), peritoneal lavage (PL), spleen (SP), and blood (BL) was determined (a-b). Ki67 staining was applied to measure the proliferation of tumor infiltrated NK1.1$^+$ cells (c).

(d-e) NK1.1 depletion antibody (clone No: PK136, 200 μg/mouse) was administrated to Ia$^+$MSCs treated B16F10 tumor bearing K$^{b-/-}$D$^{b-/-}$ mice. The efficiency of NK1.1$^+$ cell deletion (d) and the impact of NK1.1$^+$ cell deletion on tumor progression (e) were analyzed.

(f-g) Gr1 antibodies (clone No: RB6-8C5, 200 μg/mouse) and clodronate liposomes were applied to deplete myeloid cells in Ia$^+$MSCs treated B16F0 tumor bearing K$^{b-/-}$D$^{b-/-}$ mice (f). The tumor weight after Gr1 antibodies and clodronate liposomes treatment was determined (g).

Data are presented as Mean ± SEM. *p<0.05, **p<0.01, ***p<0.001, NS, no significance

# Fig. S7

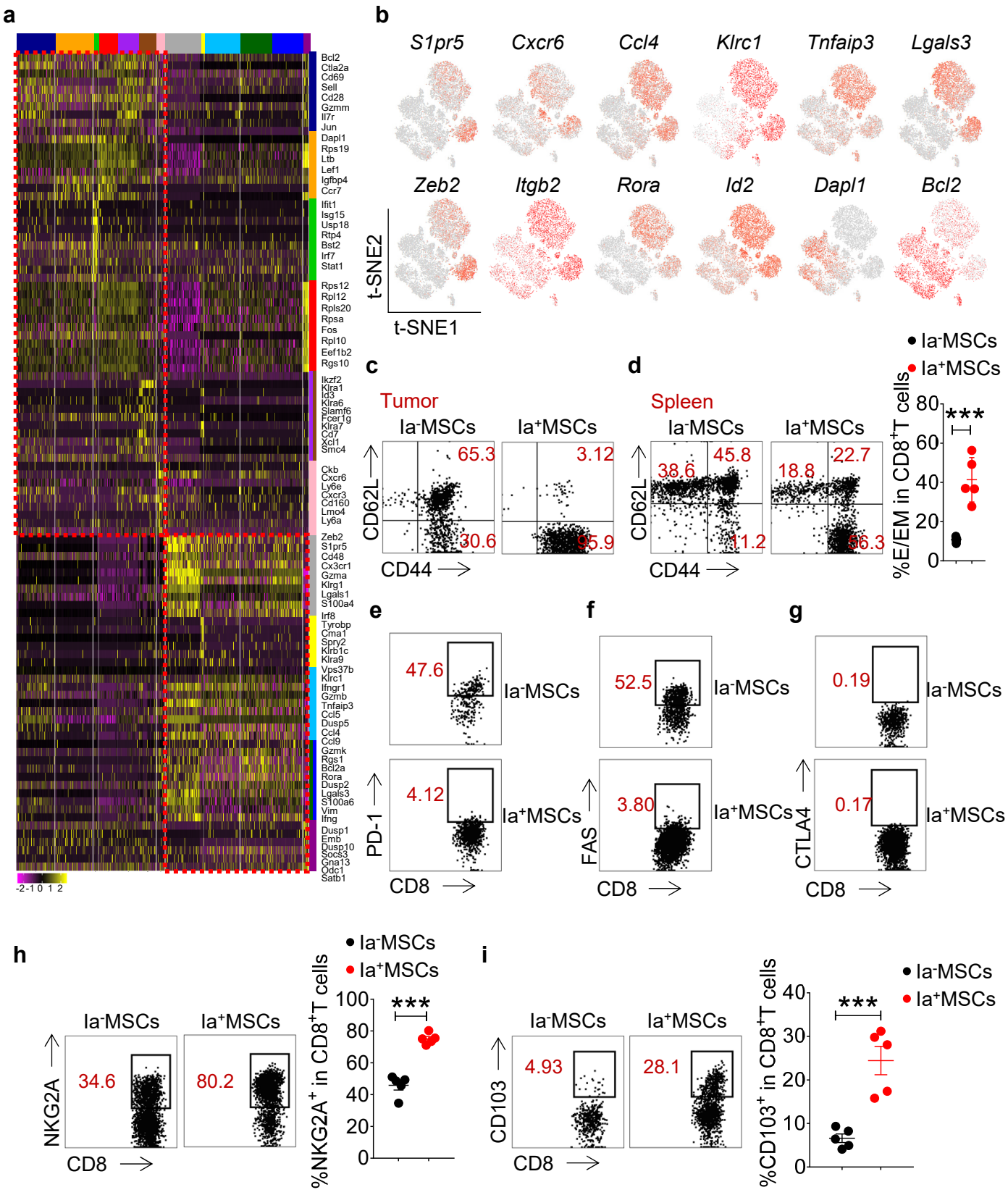
a
b
S1pr5
Cxcr6
Ccl4
Klrc1
Tnfaip3
Lgals3
Zeb2
Itgb2
Rora
Id2
Dapl1
Bcl2
t-SNE2
t-SNE1
c
Tumor
Ia-MSCs
Ia+MSCs
65.3
3.12
30.6
95.9
CD62L
CD44
d
Spleen
38.6
45.8
18.8
22.7
11.2
56.3
e
47.6
4.12
PD-1
CD8
f
52.5
3.80
FAS
g
0.19
0.17
CTLA4
h
34.6
80.2
NKG2A
%NKG2A+ in CD8+T cells
i
4.93
28.1
CD103
%CD103+ in CD8+T cells
%E/EM in CD8+T cells
***

**Fig. S7. Characterization of Ib-CD8$^+$ T cells in tumor bearing mice treated with MSCs, related to Fig. 2 and Table S1.**

(a) The unsupervised heatmap view of CD8$^+$ T cell subsets and their marker genes in Fig. 2a.

(b) Relative expression marker genes of CD8$^+$ subsets superimposed on the t-SNE projections shown in Fig. 2a.

(c-d) Ia$^-$MSCs or Ia$^+$MSCs were i.p. administrated to K$^{b-/-}$D$^{b-/-}$ mice with B16F10 i.v. inoculation. The CD44 and CD62L expression in tumor infiltrated and splenic CD8$^+$ T cells were examined. E/EM represented CD44$^+$CD62L$^-$ effector and effector memory CD8$^+$ T cells.

(e-i) Ia$^-$MSCs or Ia$^+$MSCs were i.p. administrated to K$^{b-/-}$D$^{b-/-}$ mice with B16F10 i.v. inoculation. The expression levels of PD-1 (e), FAS (f), CTLA4 (g), NKG2A (h), and CD103 (i) in tumor infiltrated CD8$^+$ T cells were examined.

Data are presented as Mean±SEM. ***p<0.001.

# Fig. S8

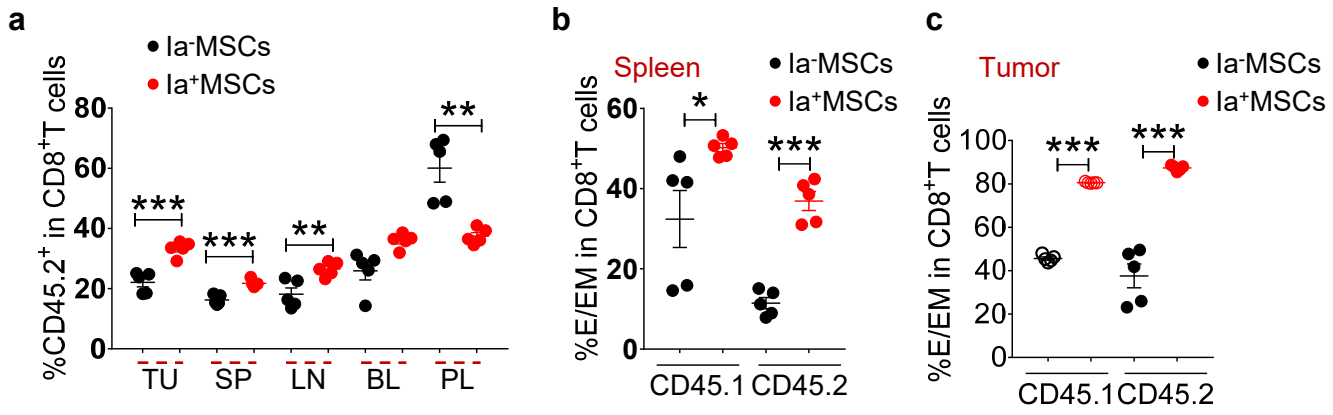


**Fig. S8. Peritoneal Ib-CD8$^+$ T cells migrate to tumor and lymphoid organs after encountering Ia$^+$MSCs, related to Fig. 2.**

(a) B16F10 tumor bearing CD45.1$^+$K$^{b-/-}$D$^{b-/-}$ mice were i.p. injected with splenocytes derived from CD45.2$^+$K$^{b-/-}$D$^{b-/-}$ mice together with Ia$^-$MSCs or Ia$^+$MSCs. The percentage of transferred CD45.2$^+$ Ib-CD8$^+$ T cells in total CD8$^+$ T cells in tumor (TU), spleen (SP), lymph node (LN), blood (BL), and peritoneal lavage (PL) were analyzed.

(b-c) The percentage of CD44$^+$CD62L$^-$ effector and effector memory (E/EM) cells in CD45.1$^+$ or CD45.2$^+$ splenic or tumor infiltrated CD8$^+$ T cells was determined by flow cytometry.

Data are presented as Mean±SEM. *p<0.05, **p<0.01, ***p<0.001.

# Fig. S9

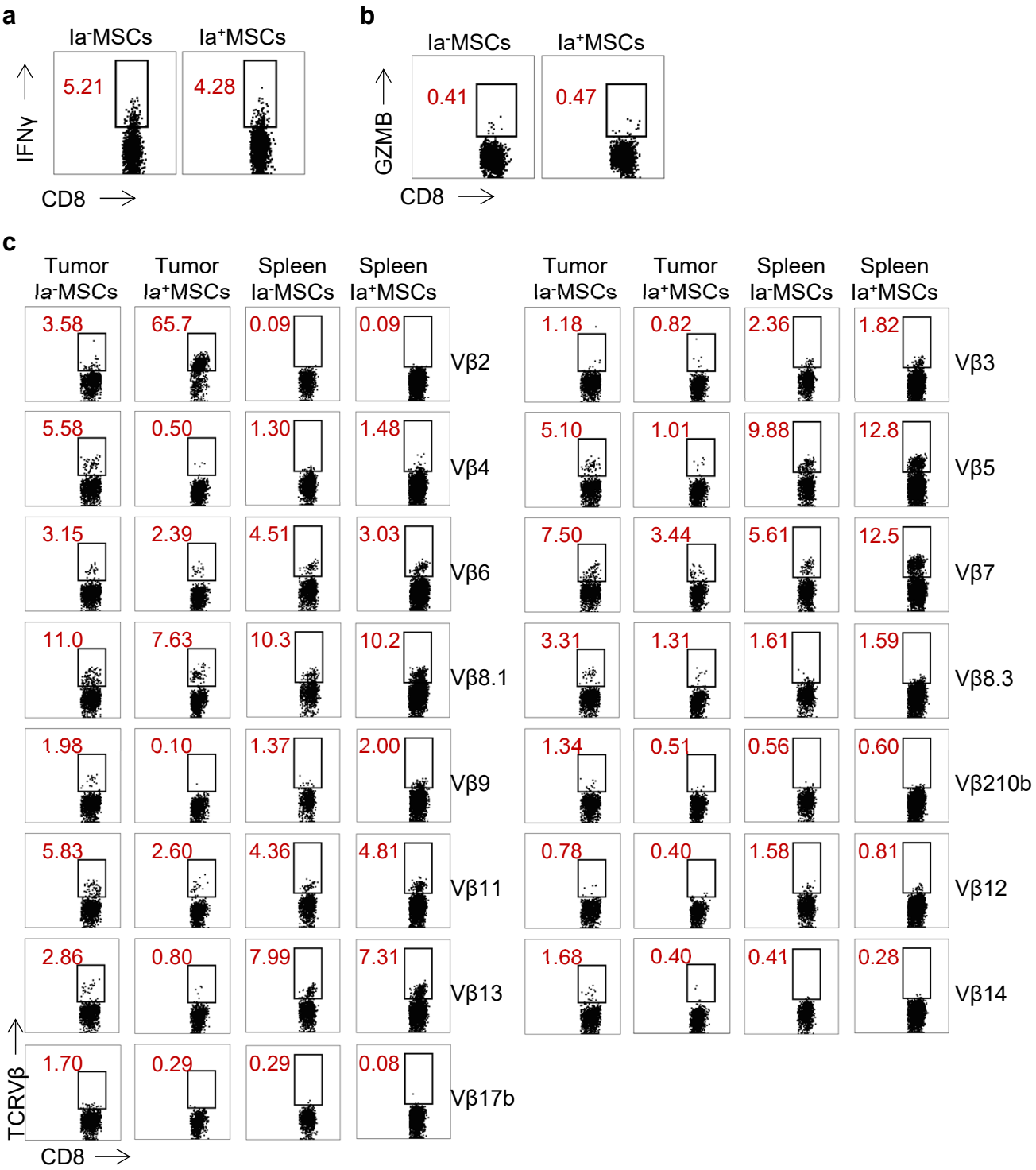


**Fig. S9. TCRvβ usage in CD8$^+$ T cells of K$^{b-/-}$D$^{b-/-}$ mice, related to Fig. 3.**

(a-b) Ia$^+$MSCs were i.p. administrated to K$^{b-/-}$D$^{b-/-}$ mice with B16F10 i.v. inoculation. The IFNγ (a) and GZMB (b) expression levels in splenic CD8$^+$ T cells were examined.

(c) K$^{b-/-}$D$^{b-/-}$ mice were i.v. injected with B16F10 cells ($3\times10^5$). The tumor bearing mice were i.p. injected with Ia$^-$MSCs ($1\times10^6$) or Ia$^+$MSCs ($1\times10^6$) every 3 days starting on day 0. After 16 days, splenic and tumor infiltrated CD8$^+$ T cells were tested for their TCRvβ usage.

# Fig. S10

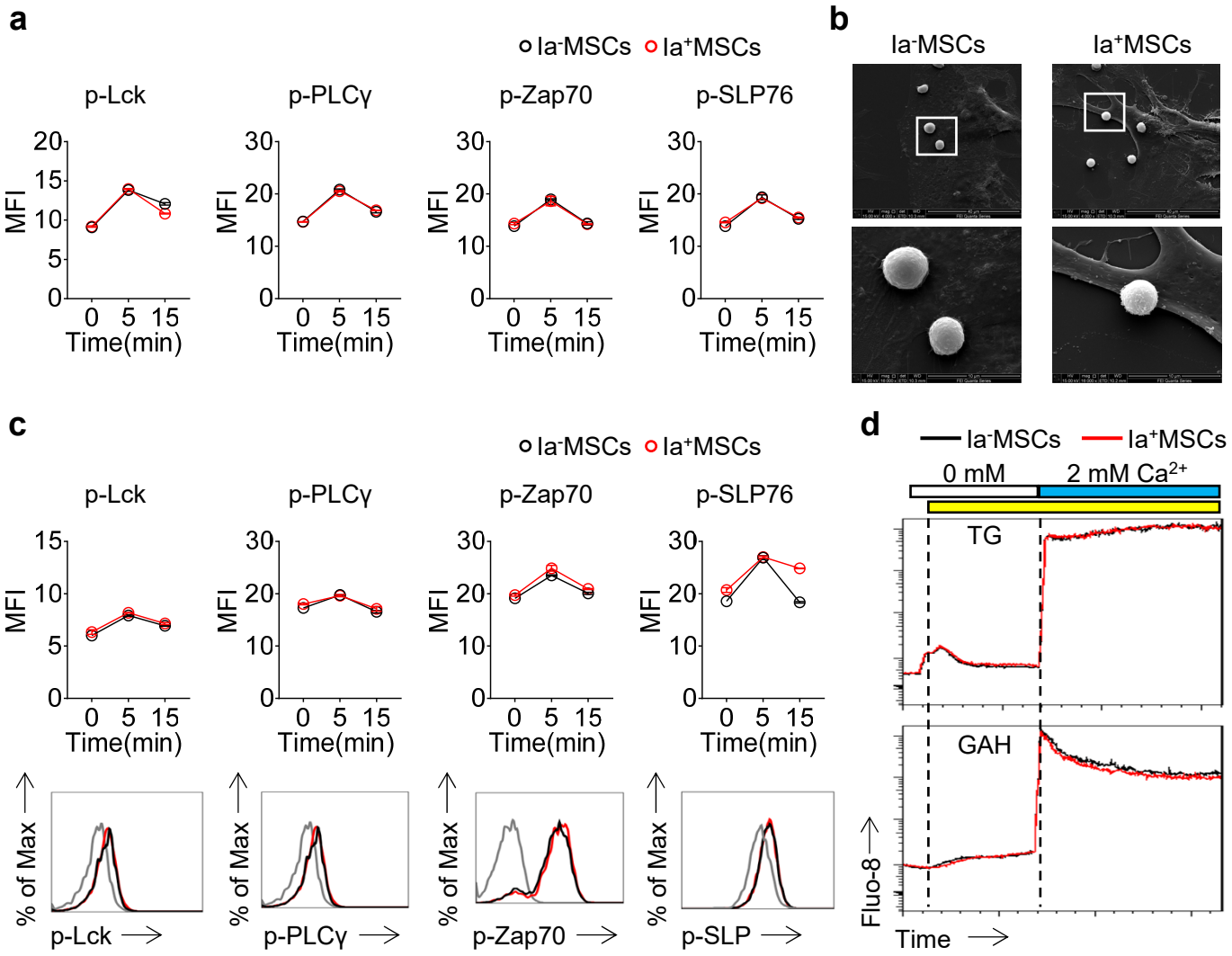


**Fig. S10. MHC Ia could not prime Ia-CD8$^+$ T cells, related to Fig. 6.**

(a) Purified CD8$^+$ T cells from C57BL/6 mice were activated in the presence of Ia$^+$MSCs or Ia$^-$MSCs. The phosphorylation of Lck, PLCγ, Zap70 and SLP76 was determined at 0, 5, and 15 min by flowcytometry.

(b) CD8$^+$ T cells were isolated from the spleen of C57BL/6 mice and co-cultured with Ia$^+$MSCs or Ia$^-$MSCs. The images by scanning electron microscopy were obtained after 24 hours co-culture.

(c) CD8$^+$ T cells from C57BL/6 mice were co-cultured with Ia$^+$MSCs or Ia$^-$MSCs for 24 hours. CD8$^+$ T cells were then separated from co-culture system and stimulated with α-CD3/CD28. The phosphorylation of Lck, PLCγ, Zap70 and SLP76 in CD8$^+$ T cells was determined. Histograms in the lower panel represents the signal intensities of phosphorylated protein after 5 min stimulation.

(d) Store-operated $Ca^{2+}$ influx in CD8$^+$ T cells from C57BL/6 mice co-cultured with Ia$^+$MSCs or Ia$^-$MSCs in response to 1 μM thapsigargin (TG; upper panel) or goat-anti-hamster IgG (GAH; lower panel) mediated crosslinking of anti-CD3 and anti-CD28 antibodies.

# Fig. S11

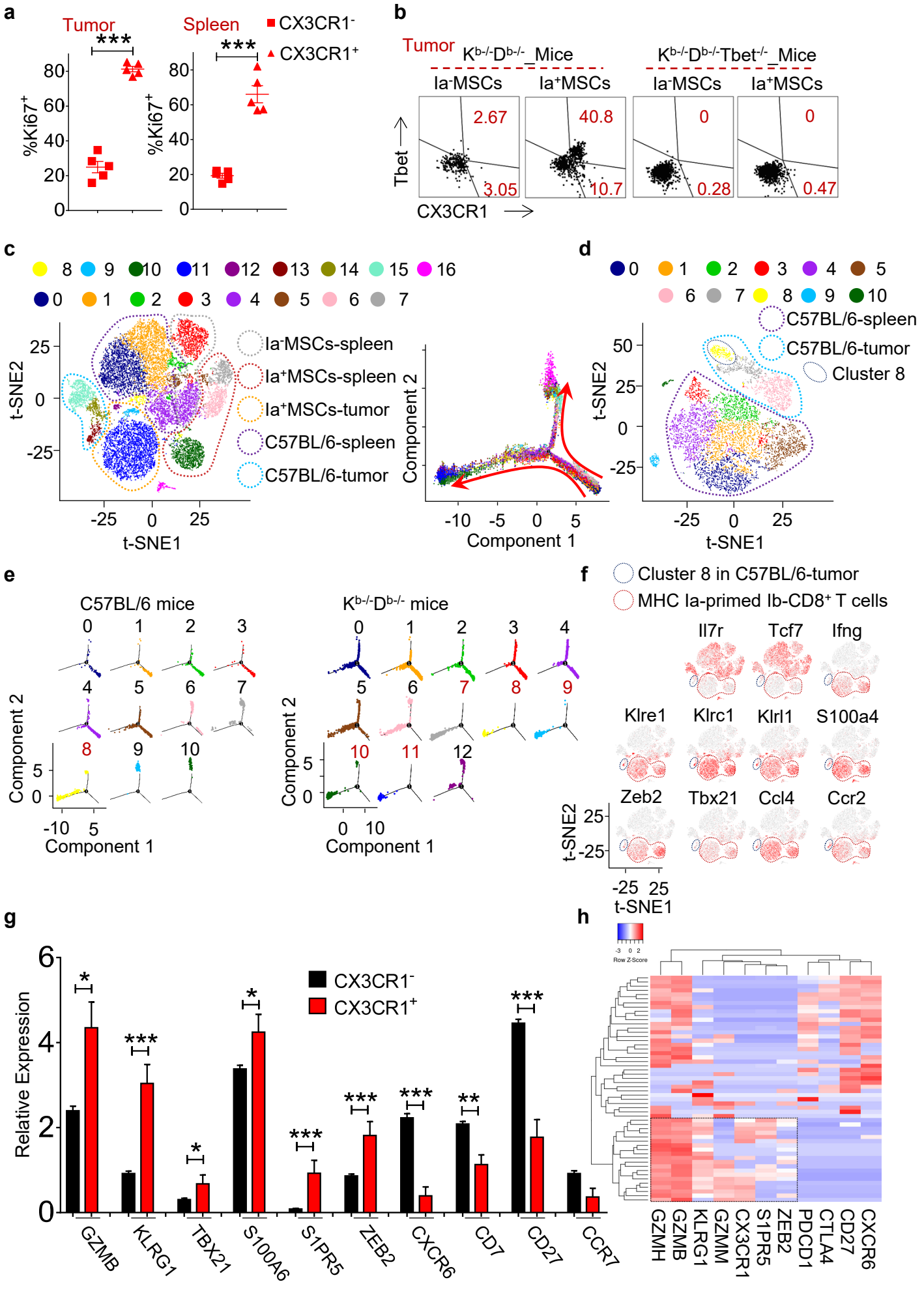
a
Tumor
Spleen
CX3CR1-
CX3CR1+
***
%Ki67+
b
Tumor
Kb-/-Db-/-_Mice
Kb-/-Db-/-Tbet-/-_Mice
Ia-MSCs
Ia+MSCs
2.67
40.8
0
0
3.05
10.7
0.28
0.47
Tbet
CX3CR1
c
Ia-MSCs-spleen
Ia+MSCs-spleen
Ia+MSCs-tumor
C57BL/6-spleen
C57BL/6-tumor
t-SNE1
t-SNE2
Component 1
Component 2
d
C57BL/6-spleen
C57BL/6-tumor
Cluster 8
e
C57BL/6 mice
Kb-/-Db-/- mice
f
Cluster 8 in C57BL/6-tumor
MHC Ia-primed Ib-CD8+ T cells
Il7r
Tcf7
Ifng
Klre1
Klrc1
Klrl1
S100a4
Zeb2
Tbx21
Ccl4
Ccr2
g
CX3CR1-
CX3CR1+
Relative Expression
GZMB
KLRG1
TBX21
S100A6
S1PR5
ZEB2
CXCR6
CD7
CD27
CCR7
h
Row Z-Score
GZMH
GZMB
KLRG1
GZMM
CX3CR1
S1PR5
ZEB2
PDCD1
CTLA4
CD27
CXCR6

**Fig. S11. Existence of tumoricidal CX3CR1$^{+}$CD8$^{+}$ T cells in wild type mice and melanoma patients, related to Fig. 6, Table S1, Table S4, Table S6, and Table S7.**

(a) In B16F10 tumor bearing $K^{b-/-}D^{b-/-}$ mice receiving Ia$^{+}$MSC administration, tumor infiltrated and splenic CD8$^{+}$ T cells were classified into two groups based on CX3CR1 expression. The percentages of Ki67 positive cells in each group were determined by flow cytometry.

(b) B16F10 tumor model was established in $K^{b-/-}D^{b-/-}$ mice and $K^{b-/-}D^{b-/-}Tbet^{-/-}$ mice by i.v injection of B16F10 cells. Ia$^{-}$MSCs ($1\times10^{6}$) or Ia$^{+}$MSCs ($1\times10^{6}$) were i.p. injected into tumor bearing mice every 3 days starting on day 0. The expression levels of CX3CR1 and Tbet in tumor infiltrated CD8$^{+}$ T cells were determined by flow cytometry.

(c) B16F10 melanoma were i.v. inoculated into C57BL/6 mice and $K^{b-/-}D^{b-/-}$ mice. $K^{b-/-}D^{b-/-}$ mice received i.p. administrated Ia$^{+}$MSCs or Ia$^{-}$MSCs every 3 days starting on day 0. On day 9, splenic CD8$^{+}$ T cells from Ia$^{-}$MSCs treated $K^{b-/-}D^{b-/-}$ mice (Ia$^{-}$MSCs-spleen), splenic or tumor infiltrated CD8$^{+}$ T cells from Ia$^{+}$MSCs treated $K^{b-/-}D^{b-/-}$ mice (Ia$^{+}$MSCs-spleen, Ia$^{+}$MSCs-tumor), as well as splenic or tumor infiltrated CD8$^{+}$ T cells from C57BL/6 mice (C57BL/6-spleen, C57BL/6-tumor) were isolated using magnet beads and subjected to single cell RNA sequencing. The t-SNE plot of the analyzed cells with their tissue origin was depicted (left panel). Pseudotime analysis of CD8$^{+}$ T cells isolated from C57BL/6 mice and $K^{b-/-}D^{b-/-}$ mice is shown (right panel).

(d) The t-SNE plot view of splenic and tumor infiltrated CD8$^{+}$ T cells isolated from C57BL/6 mice (C57BL/6-spleen, C57BL/6-tumor) was depicted.

(e) The position of each CD8$^{+}$ T cell subsets originated from either C57BL/6 mice (shown in Fig. S11d) or $K^{b-/-}D^{b-/-}$ mice (shown in Fig. 2a) in the pseudotime trajectory of total CD8$^{+}$ T cells (shown in Fig. S11c) was depicted.

(f) Relative expression intensity of selected genes superimposed on the t-SNE projections shown in (c). Those MHC Ia primed Ib-CD8$^{+}$ T cells (red dashed line) and CD8$^{+}$ T cell population in C57BL/6 mice (blue dashed line) similar to MHC Ia primed Ib-CD8$^{+}$ T cells are circled.

(g-h) Re-analysis on tumor infiltrated CD8$^{+}$ T cells derived from melanoma patients from published single cell transcriptome datasets. The average genes expression levels of CX3CR1$^{+}$ and CX3CR1$^{-}$ CD8$^{+}$ T cells were determined (g) (Tirosh et al., 2016) and the heatmap view of selected gene expression of tumor infiltrated CD8$^{+}$ T cells in melanoma patients (h) (Jerby-Arnon et al., 2018).

Data are presented as Mean±SEM. *$p<0.05$, **$p<0.01$, ***$p<0.001$.

# Fig. S12

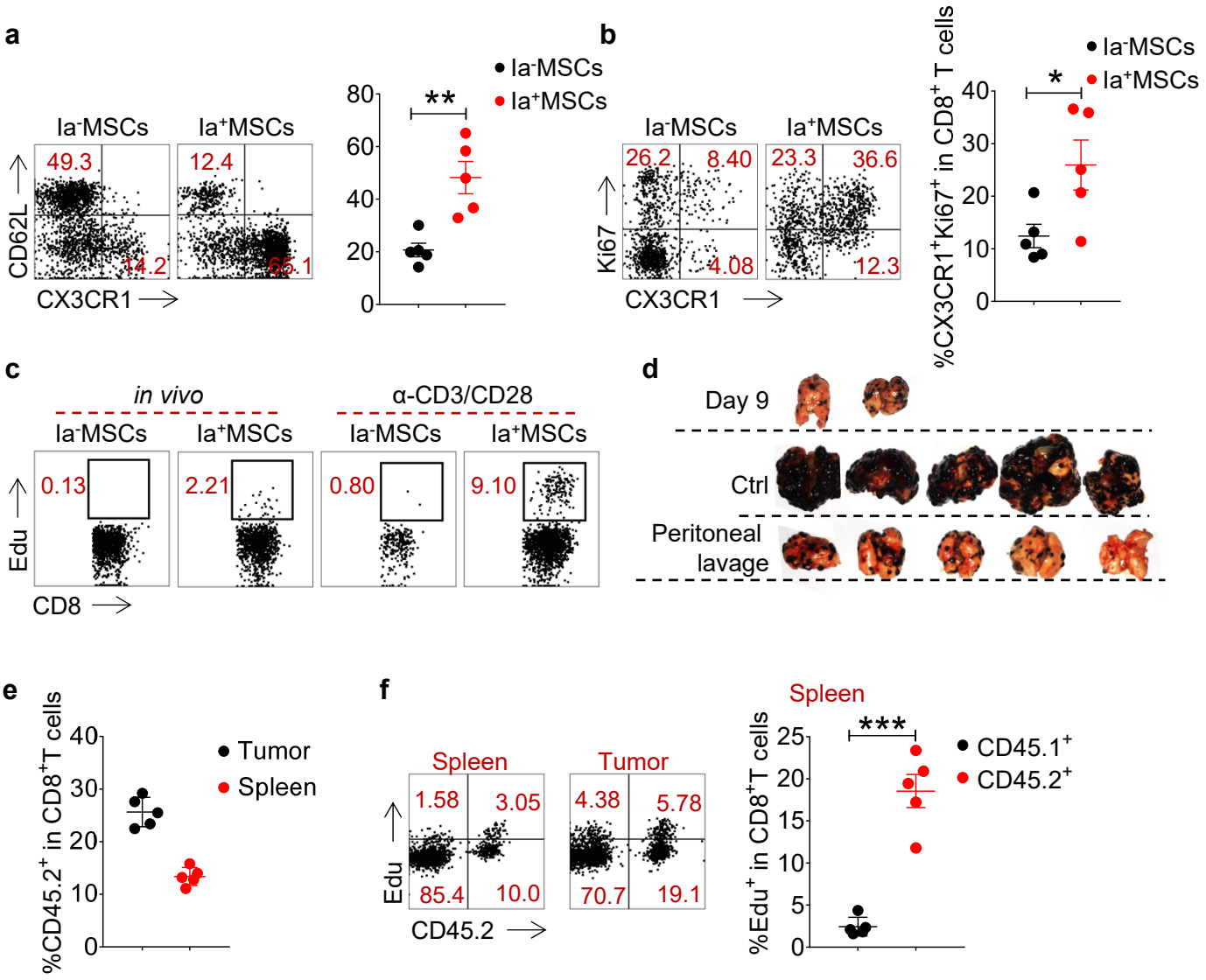


**Fig. S12. MHC Ia primed CX3CR1$^+$ Ib-CD8$^+$ T cells are enriched in peritoneal lavage, related to Fig. 6.**

(a-b) The Ki67, CX3CR1, and CD62L expression levels on CD8$^+$ T cells in the peritoneal lavages of $K^{b-/-}D^{b-/-}$ B16F10 ($3\times10^5$, i.v.) tumor bearing mice receiving i.p. injected Ia$^+$MSCs or Ia$^-$MSCs were analyzed by flow cytometry.

(c) Edu incorporation assay was applied to measure the proliferation of peritoneal CD8$^+$ T cells *in vivo*. The peritoneal CD8$^+$ T cells were isolated using magnet beads and stimulated with α-CD3/CD28 *in vitro* to evaluate their responsiveness to TCR activation.

(d-f) B16F10 cells were i.v. injected into CD45.1$^+$C57BL/6 mice and irradiated (5 Gy) on day 9. Then they received peritoneal lavage from Ia$^+$MSCs pre-treated CD45.2$^+K^{b-/-}D^{b-/-}$ mice every 3 days. The mice were euthanized on day 22 post tumor inoculation. The photograph of the lungs of CD45.1$^+$C57BL/6 mice with different treatment were shown (d). The tumor burden at the treatment time point on day 9 is also depicted (d). The reconstitution rates of CD45.2$^+$Ib-CD8$^+$ T cells in the spleen and tumor of wild type mice were determined (e). The ratio of proliferating cells among CD45.1$^+$ host CD8$^+$ T cells and CD45.2$^+$ Ib-CD8$^+$ T cells was measured by Edu incorporation assay (f).

Data are presented as Mean±SEM. *p<0.05, **p<0.01, ***p<0.001.